

Article

Efficacy Evaluation of Cu- and Ag-Based Antibacterial Treatments on Polypropylene Fabric and Comparison with Commercial Products

Nunzia Gallo ^{1,*} , Giorgia Natalia Iaconisi ² , Mauro Pollini ¹ , Federica Paladini ¹ , Sudipto Pal ^{1,3} , Concetta Nobile ⁴, Loredana Capobianco ² , Antonio Licciulli ¹, Giovanna Giuliana Buonocore ⁵, Antonella Mansi ⁶ , Luca Salvatore ¹  and Alessandro Sannino ¹

¹ Department of Engineering for Innovation, University of Salento, Via Monteroni, 73100 Lecce, Italy; mauro.pollini@unisalento.it (M.P.); federica.paladini@unisalento.it (F.P.); sudipto.pal@unisalento.it (S.P.); antonio.licciulli@unisalento.it (A.L.); luca.salvatore@unisalento.it (L.S.); alessandro.sannino@unisalento.it (A.S.)

² Department of Biological and Environmental Sciences and Technologies, University of Salento, Via Monteroni, 73100 Lecce, Italy; giorgianatalia.iaconisi@unisalento.it (G.N.I.); loredana.capobianco@unisalento.it (L.C.)

³ Nanohub, Via Verdi 8, Bodio Lomnago, 21020 Varese, Italy

⁴ CNR Nanotec, Institute of Nanotechnology, Via Monteroni, 73100 Lecce, Italy; concetta.nobile@nanotec.cnr.it

⁵ CNR, Institute of Polymers, Composites and Biomaterials (IPCB), Piazzale E. Fermi, 80055 Naples, Italy; gbuonoco@unina.it

⁶ Department of Occupational and Environmental Medicine, Epidemiology and Hygiene, Italian Workers' Compensation Authority (INAIL), Via Fontana Candida 1, Monte Porzio Catone, 00078 Rome, Italy; a.mansi@inail.it

* Correspondence: nunzia.gallo@unisalento.it



Citation: Gallo, N.; Iaconisi, G.N.; Pollini, M.; Paladini, F.; Pal, S.; Nobile, C.; Capobianco, L.; Licciulli, A.; Buonocore, G.G.; Mansi, A.; et al. Efficacy Evaluation of Cu- and Ag-Based Antibacterial Treatments on Polypropylene Fabric and Comparison with Commercial Products. *Coatings* **2023**, *13*, 919. <https://doi.org/10.3390/coatings13050919>

Academic Editor: Liqun Xu

Received: 31 March 2023

Revised: 5 May 2023

Accepted: 11 May 2023

Published: 14 May 2023



Copyright: © 2023 by the authors. Licensee MDPI, Basel, Switzerland. This article is an open access article distributed under the terms and conditions of the Creative Commons Attribution (CC BY) license (<https://creativecommons.org/licenses/by/4.0/>).

Abstract: Filter masks are disposable devices intended to be worn in order to reduce exposure to potentially harmful foreign agents of 0.1–10.0 microns. However, to perform their function correctly, these devices should be replaced after a few hours of use. Because of this, billions of non-biodegradable face masks are globally discarded every month (3 million/minute). The frequent renewal of masks, together with the strong environmental impact of non-biodegradable plastic-based mask materials, highlights the need to find a solution to this emerging ecological problem. One way to reduce the environmental impact of masks, decrease their turnover, and, at the same time, increase their safety level is to make them able to inhibit pathogen proliferation and vitality by adding antibacterial materials such as silver, copper, zinc, and graphene. Among these, silver and copper are the most widely used. In this study, with the aim of improving commercial devices' efficacy and eco-sustainability, Ag-based and Cu-based antibacterial treatments were performed and characterized from morphological, compositional, chemical–physical, and microbiological points of view over time and compared with the antibacterial treatments of selected commercial products. The results demonstrated the good distribution of silver and copper particles onto the surface of the masks, along with almost 100% antibacterial capabilities of the coatings against both Gram-positive and Gram-negative bacteria, which were still confirmed even after several washing cycles, thus indicating the good potential of the developed prototypes for mask application.

Keywords: antibacterial treatment; silver nanoparticles; copper nanoparticles; mask; medical device; personal protective equipment; community face covering

1. Introduction

Filter masks, or simply masks, are disposable devices intended to be worn in order to reduce exposure to potentially harmful foreign agents of dimensions between 0.1 and 10 microns (i.e., dust, fine dust, fumes, mists, bacteria, and viruses). In particular, it is widely known that some pathogens (i.e., bacteria and viruses) are air-transmitted via

the droplets (>5 microns) and aerosols (<5 microns) of respiratory secretions, which are emanated during normal breathing, conversation, and in large quantities in the case of coughing and sneezing [1].

Actually, there are different types of masks whose design and material depend on their filtering power and use [2]. Obviously, these characteristics strongly influence the level of protection against the spread of airborne diseases. Thus, masks are divided into three categories [3]: (i) surgical masks, that fall within the category of medical devices (DM), which protect the wearer from contamination by operators, according to the UNI EN 14683:2019 + AC:2019 [4]; (ii) filtering facepieces, that are included in the category of personal protective equipment (PPE), which protect operators from external contamination, according to the UNI EN 149:2009 [5]; and (iii) community face coverings (CFC), that are designed to make up for the lack of DM and PPE during the COVID-19 pandemic or to combat excessive smog in areas with a high rate of pollution and are actually produced and commercialized, according to the PdR UNI 90:2020 [6].

The use of masks, therefore, would allow us to limit the interaction of human airways with harmful foreign agents. However, to perform their function correctly, these devices should be replaced after a few hours [2,7]. Because of this, about 129 billion non-biodegradable face masks are globally used every month (3 million/minute) [8]. The frequent renewal of masks, together with the strong environmental impact of non-biodegradable mask materials, highlights the need to find a solution to this emerging ecological problem [3,9,10].

One way to reduce their environmental impact, decrease their turnover, and increase their safety level is to make masks not only able to prevent the entry of pathogens but also able to inhibit their proliferation (bacteriostatic action) and vitality (bactericidal action). For example, many studies proved the presence of SARS-CoV-2 on masks' inner and outer layers for more than four days, suggesting that contaminated masks became pathogen transmission sources [11]. Moreover, one of the most important problems arising from the use of DM and PPE was the accumulation of breathing moisture that, together with body temperature (35–37 °C), promoted pathogen accumulation and growth. Therefore, to reduce the bacterial population and minimize pathogenic infections, masks with antibacterial properties were developed [7,12,13]. The addition of an antimicrobial agent could not only increase masks' safety level but also increase their use time, making them eco-friendlier and more effective. Moreover, these factors make it possible to limit their daily use and, thus, their cost to the community. Consequently, a huge reduction in plastic disposal could be achieved. Therefore, antimicrobial fabrics and related antibacterial masks are currently of great interest, with a rapidly increasing market value. Worldwide, several companies have started to produce CFC, MD, or PPE with antibacterial properties.

The bacteriostatic/bactericidal activity was generally provided by the addition, through various techniques, of materials with known antibacterial properties such as silver, copper, zinc, and graphene [1,7,13–16]. Among these, silver and copper are bacteriostatic/bactericidal materials par excellence and have been used since ancient times for their antiviral and antibacterial properties [14,17–21]. Indeed, several studies showed how colloidal silver and copper (in pure form or in alloys) were able to minimize the proliferation of numerous species of microorganisms (viruses, bacteria) in little time [7,15,21–28].

In this study, with the aim of improving commercial devices' efficacy and eco-sustainability and extending their duration of use, two prototypes of face masks were developed by performing Ag-based or Cu-based antibacterial treatments on polypropylene (PP) fabrics. Among several kinds of antibacterial agents, silver and copper were chosen for their known efficacy and well-documented action mechanisms [20,29–35]. PP has been defined as the ideal fibrous material to produce face mask textiles due to its low cost, mechanical strength, and chemical resistance [1]. Providing a bacteriostatic and/or bactericidal activity to PP fabrics would give high added value to masks, greatly enhancing their protective efficacy. Therefore, the development of surface antibacterial treatments for PP surgical masks could be of considerable interest, as they will be able to maintain their

filtering power unaltered, increase the level of safety they offer, and decrease their turnover and disposal.

The two prototypes we developed were characterized from a morphological, compositional, chemical–physical, and microbiological point of view and compared with the antibacterial treatments of selected commercial products. The surface morphology of the two prototypes, along with their antibacterial treatment, spatial distribution, and elemental composition, were observed using scanning electron microscopy (SEM) in combination with X-ray energy dispersive spectroscopy (XEDS). The percentage of Ag or Cu that was incorporated was gravimetrically obtained. The water-repellent character of the treatments was evaluated by contact angle measurements. The crystal structure of Ag or Cu nanoparticles on the fabric was investigated by X-ray diffraction (XRD). The effectiveness of the antibacterial treatment against Gram-negative (i.e., *Escherichia coli*) and Gram-positive (i.e., *Staphylococcus aureus*) bacteria was assessed according to the AATCC Standard Test Method 100 (1993) from the AATCC Technical Manual. Finally, the same analyses were performed to evaluate the masks' durability during washings and drying cycles.

2. Materials and Methods

2.1. Materials

The PP fabric used for Ag- and Cu-based antibacterial treatments was collected from the IIR surgical masks commercialized by Sicura Protection (Vibo Valentia, Italy). Commercial mask samples were kindly provided by Olvitech (Modi'in-Maccabim-Re'ut, Israel), ARGO Industries (Chippenham, UK), Respilon (BRNO, Czech Republic), Absolutex (Vittorio Veneto, Italia) and Primeway (Maharashtra, India). Silver nitrate (ACS reagent, $\geq 99.0\%$) as precursor for silver nanoparticles and methanol (ACS reagent, $\geq 99.8\%$) as photo-reducing agent were purchased from Sigma Aldrich. Copper nanoparticle (CuNC)-based face masks were prepared using copper acetate monohydrate ($[\text{Cu}(\text{CH}_3\text{COO})_2 \cdot \text{H}_2\text{O}]$, 98%, Sigma-Aldrich) and hydrazine hydrate ($\text{N}_2\text{H}_4 \cdot \text{H}_2\text{O}$; 50–60%, Sigma-Aldrich) as the starting precursors. All chemicals were used without modifications. Distilled water was obtained from Millipore Milli-U10 water purification facility from Merck KGaA (Darmstadt, Germany). *Escherichia coli* (ATCC®25922) and *Staphylococcus aureus* (ATCC®29213) were purchased from Mecconti Sarl (Warsaw, Poland). All other chemicals used were of analytical grade and purchased from Sigma-Aldrich (St. Louis, MO, USA).

2.2. Antibacterial Treatments Development

The PP fabric (thickness: $120 \pm 15 \mu\text{m}$) was subjected to two antibacterial treatments: Ag-based and Cu-based.

The silver treatment was performed by using a technology based on in situ photo-chemical deposition of silver particles onto the surface of the material. The process involves different stages, namely (i) preparation of the impregnating silver solution; (ii) deposition of the silver solution through dip or spray coating onto the substrate; (iii) UV exposure; (iv) washing. For this specific material and application, the silver solution was prepared by mixing 2 wt/wt% AgNO_3 , 20 wt/wt% CH_3OH , and 78 wt/wt% deionized water under magnetic stirring for 30 min at room temperature. Then, the silver solution was deposited by dip coating onto the substrate, which was subsequently exposed to a UV lamp (Jelosil HG 200 ULTRA, peak at $\lambda = 365 \text{ nm}$, distance 30 cm) for 15 min in order to allow the synthesis and adhesion of the Ag particles onto the fabric. Finally, the silver-nanoparticle-enriched PP fabric (SIL, thickness $144 \pm 5 \mu\text{m}$) was washed to remove any residual trace of silver nitrate, dried at room temperature, and stored until use.

Copper nanoparticles were deposited on the PP fabric, following our previous work with little modification [36]. Briefly, a 0.3% (*w/v*) aqueous Cu solution was prepared by dissolving the required amount of copper acetate in 100 mL of distilled water. After the copper salt was fully dissolved, four pieces of PP fabric (approx. $2 \text{ cm} \times 4 \text{ cm}$) were placed in the solution with vigorous stirring, followed by dropwise addition of the reducing agent (hydrazine hydrate, 5 mL/100 mL water). The stirring continued for 8 h, and after that, the

fabric was washed three times with distilled water. Then, copper-nanoparticle-enriched PP fabric (COP, thickness $160 \pm 10 \mu\text{m}$) was dried at room temperature and stored for further use.

2.3. Identification and Selection of Mask Commercial Samples

The commercial masks that are available in the national and international market were collected from the search engine Google. The keywords used in the search engine were ‘mask’, ‘antibacterial’, ‘silver’, and ‘copper’. Moreover, some synonyms (e.g., face covering, filter mask, surgical mask, dust mask, protective mask, facial, DM, PPE, and CFC) were searched.

Products for inclusion were selected in two stages. Firstly, data on the antibacterial treatment type, the product name, and the company name, were collected and reviewed. Samples without clear information about the applied antibacterial treatments were excluded from the selection. Then, a more detailed data collection focused on the presence of certifications, compliance with current regulations, or reports of biocompatibility, antibacterial tests, and technical data sheets. Commercial masks that met the inclusion criteria were selected for comparative analysis. A total of 100 commercial products with antibacterial properties were screened, and five commercial masks were selected (Table 1). In regard to surgical masks, ‘Copper Oxide Medical Mask’ by Olvitech (OLV, thickness: $274 \pm 12 \mu\text{m}$) was chosen as Cu-treated DM-certified product. To the best of our knowledge, no Ag-treated DM-certified commercial products are available. In regard to PPE, ‘FFP2 Washable mask’ by ARGO Industries (ARG, thickness: $587 \pm 60 \mu\text{m}$) was chosen as Ag-treated PPE-certified product, while ‘VK RespiPro’ by Respilon (RES, thickness: $339 \pm 33 \mu\text{m}$) was chosen as Cu-treated PPE-certified product. In regard to CFC, ‘ACM’ by Absolutex (ABS, thickness: $361 \pm 87 \mu\text{m}$) was chosen as Ag-treated CFC, while ‘P29’ by Primeway (PRI, thickness: $626 \pm 76 \mu\text{m}$) was chosen as Cu-treated CFC.

Table 1. Mask sample types. The prototypes of Ag- and Cu- treated PP fabrics, developed by the DII of the University of Salento, were tested in comparison with commercial products of DM, PPE, and CFC.

Mask Type	Antibacterial Treatment	Company	Product Name	Code	Material
Prototypes	Silver	Unisalento	Ag	SIL	PP
	Copper	Nanohub/Unisalento	Cu	COP	PP
Surgical mask	Silver	–	–	–	–
	Copper	Olvitech	Copper Oxide Medical Mask	OLV	PP
Personal Protective Equipment	Silver	ARGO Industries	FFP2 Washable mask	ARG	Cotton/PE
	Copper	Respilon	VK RespiPro	RES	PP
Community face covering	Silver	Absolutex	ACM	ABS	PE
	Copper	Primeway	P29	PRI	PU

The antibacterial layer, identified from information reported in the technical data sheet, was harvested from each commercial mask sample and fully characterized in comparison with the Ag and Cu prototypes. In particular, the antibacterial layer was harvested from the external layer of the mask (i.e., the layer that makes contact with the external environment) for ABS and PRI, from the middle layer of the mask (i.e., the filtering unit) for ARG, and from both external and inner layers of the mask (i.e., the layers that make contact with the external environment and the skin, respectively) for OLV and RES.

The durability of the antibacterial treatments was evaluated in triplicate for each sample type after 0, 3, and 10 washing cycles at $30 \text{ }^\circ\text{C}$ for 2 h on mask samples of about $10 \text{ cm} \times 10 \text{ cm}$, using a Candy washing machine, model RP4476BWMR/1-S, (Candy S.p.a,

Milan, Italy) followed by drying cycles with an Electrolux dryer, model EW9H297DY (AB Electrolux, Stockholm, Sweden), for 2 h.

2.4. Morphological and Elemental Analysis

SEM combined with XEDS techniques was performed to investigate masks' surface morphology and the presence of antibacterial treatments. Such morphological and elemental analyses were carried out on the mask samples after 0 (0 W), 3 (3 W), and 10 (10 W) washing cycles. Thus, mask samples of about 1 cm × 1 cm were stuck to adhesive carbon tape on SEM stubs for both imaging and chemical compositional measurements. The as-prepared samples were then transferred into a field emission SEM microscope (SIGMA 300VP, Carl ZEISS, Germany, GmbH) equipped with fully integrated detectors for secondary and backscattered electrons, available both in high vacuum and in variable pressure (VP) mode, with the latter using nitrogen as imaging gas for non-conductive specimens. SEM images of the samples were recorded at HV of 20 kV and a VP of 30 Pa, with a few seconds of image integration time to minimize charging effects of the samples and to increase the image quality. ImageJ processing software (National Institute of Health, Bethesda, MD, USA) was used to measure the microfiber diameter distributions. Finally, to confirm the presence of the antibacterial treatments (Ag or Cu) and, eventually, their modifications when undergoing a certain fixed number of washing cycles, EDS spectra were recorded using an SEM microscope (Merlin, Carl ZEISS, Germany, GmbH) at 20 kV, equipped with an EDS detector (Quantax, XFlash 6160, Bruker, Billerica, MA, USA) for microanalysis. The mass fractions of various chemical components were evaluated relative to carbon as a reference element, considering that C is the main dominant element of the fibers of all samples. The latter, moreover, stuck to adhesive carbon tape for electron microscopy analyses. The test was performed in triplicate for each sample type.

2.5. Crystalline Structures Investigation

The XRD analyses on fabrics were performed in order to investigate the crystalline nature of Ag or Cu nanoparticles. The XRD patterns were recorded on a Rigaku Ultima diffractometer with Cu K α radiations operating at 40 kV/20 mA on mask samples of about 1 cm × 1 cm. Samples were tested in triplicate.

2.6. Hydrophobicity Degree

Static contact angle measurements were conducted to achieve information about the surface hydrophobic character. Thus, static contact angle measurements were performed dropping 10 μ L milli-Q water on 1 cm × 1 cm samples at 25 °C using the sessile drop method with a FTA1000 tensiometer (First Ten Angstroms, Newark, NJ, USA) equipped with an X-Y syringe and a high-performance camera to capture high-resolution images [37]. The contact angle values were quantified using the tensiometer software. The test was performed six times for each sample type.

2.7. Antibacterial Agent Content

The antibacterial agent content was quantified before and after the washing cycles, and it was correlated with masks' antibacterial activity. The quantitative evaluation of the Ag or Cu content before and after washing cycles was performed gravimetrically. Briefly, mask samples of about 3 cm × 3 cm were sealed in alumina crucibles and heated up to 600 °C for 18 h. The solid residue quantified at the end of the test represented the incombustible Ag or Cu nanoparticles. Thus, the Ag or Cu content (C%) was calculated according to the following equation:

$$C\% = \frac{W_f}{W_i} 100, \quad (1)$$

where W_f is the dry residue of the sample after burning, and W_i is the initial weight of the mask sample. Samples were tested in triplicate.

2.8. Antibacterial Activity

The antibacterial activity of mask samples was checked against the Gram-negative *E. coli* (ATCC®25922) and the Gram-positive *S. aureus* (ATCC®29213) according to the AATCC Standard Test Method 100 (1993) from the AATCC Technical Manual [38], with some modifications. Both bacterial strains were overnight propagated at 37 ± 1 °C in Luria-Bertani (LB) broth (1% tryptone, 0.5% yeast extract, 1% NaCl) and then diluted to 4×10^6 colony-forming units (CFU)/mL in 10 mL of 0.1% Tween 80 and 0.01% Triton X-100. Before testing, control (PP fabric) and mask samples of 1 cm × 1 cm were sterilized by autoclave (121 °C, 20 min, $p = 1$ bar) and laid down into individual hermetically sealable vials. Then, 10 µl of the microbial suspension was pipetted onto the mask samples. After 1 h of incubation (37 °C, humidity of >90%), bacteria were recovered by adding 10 mL of 0.1% Tween 80 and vortexing for 1 min. Then, 10 µL was plated on LB-agar. The number of CFU/mL was determined after 24 h of incubation at 37 ± 1 °C and relative humidity >90%. According to the AATCC100, the microbial titer reduction (R%) was calculated as [38]:

$$R\% = \frac{C_i - C_f}{C_i} 100, \quad (2)$$

where C_i is the bacterial concentration (CFU/mL) recovered from the inoculated untreated fabric, and C_f is the bacterial concentration (CFU/mL) recovered from the inoculated antibacterial fabric after 1 h of incubation. The test was performed in quadruplicate.

2.9. Statistical Analysis

All data were expressed as mean ± the standard deviation. Statistical significance of all experimental data was determined using Student's t-test. Differences were considered significant at $p < 0.05$.

3. Results

3.1. Morphological and Elemental Analysis

SEM and EDS analyses were performed to assess the micro-fiber morphology as well as to confirm the presence of the antibacterial nanomaterials (either Ag or Cu) before and after washing cycles.

The PP fabric used for Ag and Cu treatments was characterized by randomly oriented fibers. The mean fiber diameter of SIL and COP was found to be about 5.0 ± 2.7 µm. However, it should be noted that the fiber distribution slightly changed after three washing cycles and even more markedly after ten cycles (Figure 1). Given that the image contrast of a metal, like Ag or Cu, is much sharper than that of the fabric material, the SEM analysis also gave clear indications of the presence of Ag and Cu antibacterial treatments in SIL and COP samples, respectively. Actually, differences in Ag and Cu cluster distribution were detectable in both of the two different types of samples, SIL and COP. SIL was characterized by a substantial presence and the homogeneous distribution of the Ag clusters, which was not observably reduced after repeated washing cycles (Figure 1a–c). The durability of the Ag treatment was also found in the elemental analysis, as it can be inferred by the EDS data reported in Table 2. A similar PP fabric functionalization was performed by Valdez-Salas et al., who, by electrochemical deposition, obtained a well-homogenized Ag nanoparticle distribution with slight nanoparticle conglomerations [12]. An even more uniform distribution was obtained by Gawish et al., with an Ag% similar to our work [39].

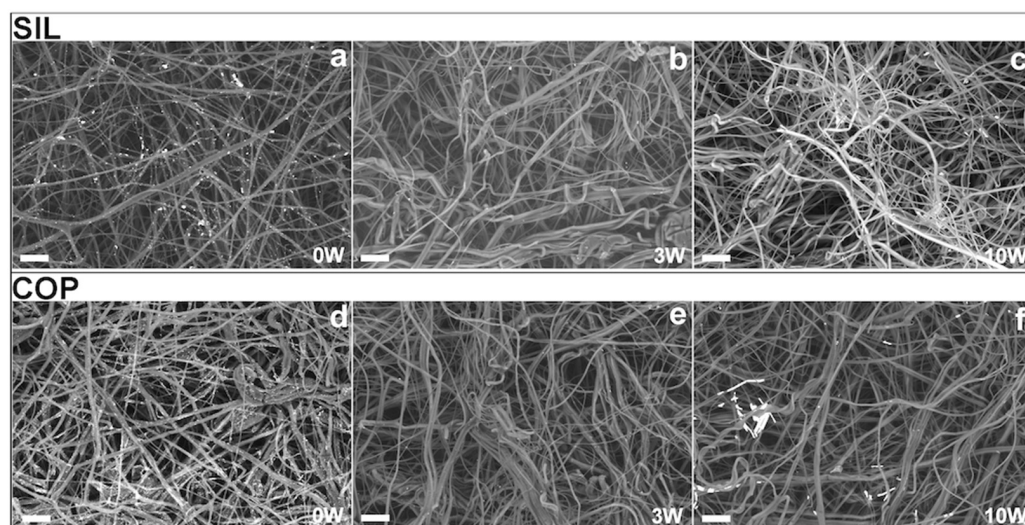


Figure 1. SEM images of the prototypal SIL (a–c) and COP (d–f) antibacterial fabric, before and after washing cycles. Scale bar: 50 μ m.

Table 2. EDS results of the prototypal and commercial antibacterial fabric before and after washing cycles.

Sample	0 W	3 W	10 W
SIL	2.61 \div 2.83%	2.45 \div 2.52%	2.44 \div 2.48%
COP	6.47 \div 6.89%	1.16 \div 1.75%	1.51 \div 1.65%
ARG	0.21 \div 0.29%	0.20 \div 0.28%	0.01 \div 0.03%
ABS	0.92 \div 1.06%	0.55 \div 0.63%	0.31 \div 0.39%
OLV	0.90 \div 1.02%	0.74 \div 0.86%	0.74 \div 0.76%
RES	1.62 \div 1.68%	1.42 \div 1.58%	0.84 \div 0.96%
PRI	0.30 \div 0.40%	0.25 \div 0.35%	0.20 \div 0.30%

For the SIL sample, the Ag mass fraction, relative to that of C, was about $\approx 2.7\%$, $\approx 2.48\%$, and $\approx 2.46\%$ at 0 W, 3 W, and 10 W cycles, respectively (Table 2), thus indicating a slight loss of silver only after the initial washing cycles. On the other hand, COP was also characterized by a high coverage with the Cu-based treatment (Figure 1d). Cu coverage was found to be homogeneously distributed and similar to the work of Zhu et al., despite the different production technology [40]. However, after the washing cycles, the great part of the Cu treatment was removed, leaving some fibers coated by copper clustered in micron-sized agglomerates (Figure 1e,f), as was also confirmed by the EDS spectra of COP, which showed a drastic reduction of relative Cu mass fraction when passing from 0 W ($\approx 6.4\%$) through 3 W ($\approx 1.6\%$) and finally to 10 W ($\approx 1.5\%$) (Table 2).

Great differences were found in commercial masks (Figures 2 and 3). Figure 2 shows the results of the morphological and elemental analyses conducted on the inner antibacterial layer of the PPE ARG and the outer layer of the CFC ABS, which were both treated with silver. SEM images (Figure 2a–c) of the ARG sample clearly highlighted fibers with a larger diameter size (about $26.4 \pm 2.7 \mu\text{m}$) and a fiber net, featuring the fabric, which became more and more loose as the washing cycles increased. Furthermore, considerations concerning the SEM image contrast accounted for the poor presence of Ag nanoparticles. This was further confirmed by EDS analyses, which showed a very low percentage of Ag mass fraction relative to C fraction (0 W: $\approx 0.24\%$; 3 W: $\approx 0.25\%$; 10 W: $\approx 0.0\%$) (Table 2). Concerning ABS (mean fiber diameter $10.6 \pm 2.3 \mu\text{m}$), SEM measurements underlined the compactness of the fiber net, which became slightly looser just after 10 W and presented some residuals of fiber pieces (Figure 2d–f). An SEM overview also indicated the presence of relatively small Ag nanoparticles, and the EDS analyses carried out on the ARG samples

at 0 W, 3 W, and 10 W, accounted for a decreasing trend of the Ag mass fraction (0 W: $\approx 1.0\%$; 3 W: $\approx 0.60\%$; 10 W: $\approx 0.35\%$) (Table 2).

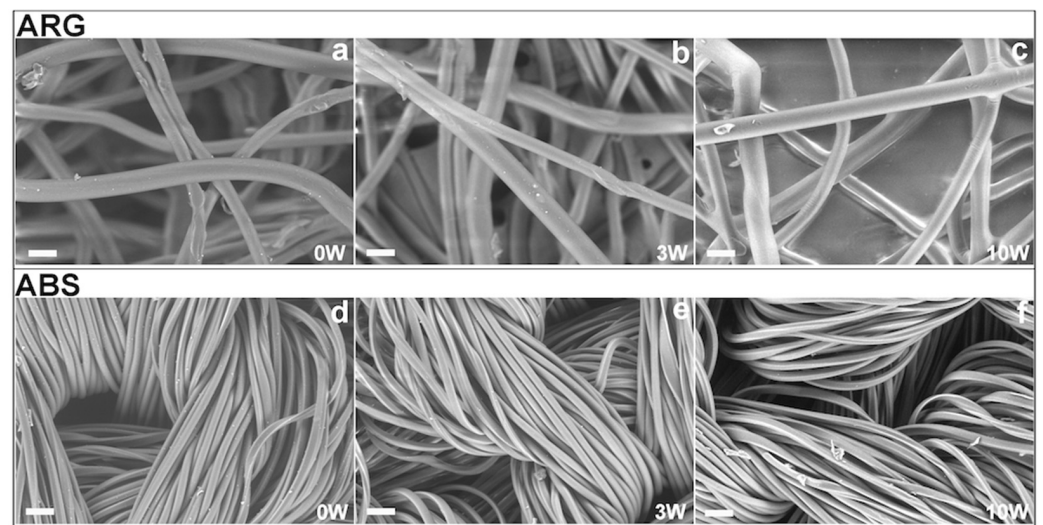


Figure 2. SEM images of the commercial ARG (a–c) and ABS (d–f) antibacterial fabric, before and after washing cycles. Scale bar: 50 μm .

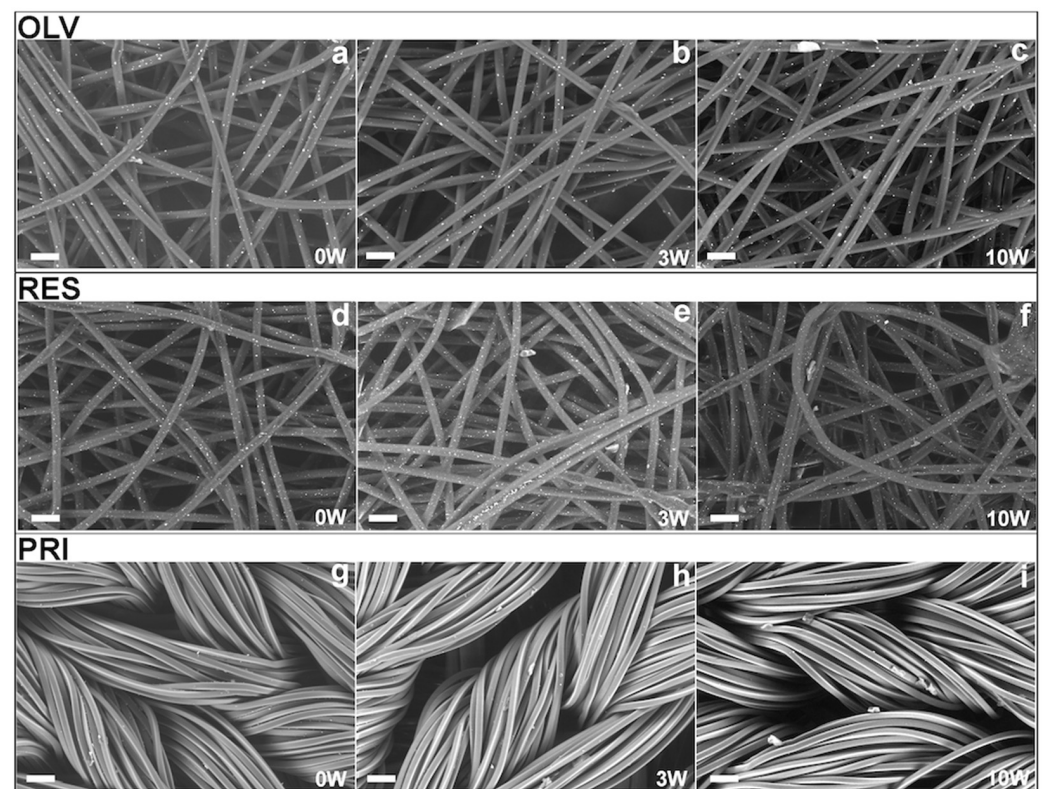


Figure 3. SEM images of the commercial OLV (a–c), RES (d–f) and PRI (g–i) antibacterial fabric, before and after washing cycles. Scale bar: 50 μm .

The SEM and EDS measurements carried out on the last three investigated commercial Cu-treated masks (i.e., the outer layers of the MD OLV, the PPE RES, and the P29 PRI) are reported in Figure 3. The OLV (Figure 3a–c) and RES (Figure 3d–f) fabrics presented some common features in terms of the compactness of the fiber net and the mean diameter size of the microfibers (OLV, $\approx 15.4 \pm 1.0 \mu\text{m}$ and RES, $\approx 15.8 \pm 0.8 \mu\text{m}$). Moreover, a substantial

invariability not only of fiber morphology but also of the homogeneous distribution of Cu-based antibacterial nanoparticles, even after 10 washing cycles, was observed. Additionally, an almost constant trend in the relative Cu mass fraction was confirmed by elemental analyses for both OLV (0 W: $\approx 0.95\%$; 3 W: $\approx 0.80\%$; 10 W: $\approx 0.80\%$) and RES (0 W: $\approx 1.7\%$; 3 W: $\approx 1.5\%$; 10 W: $\approx 0.90\%$) (Table 2). This was different in the case of PRI (Figure 3g–i), whose fiber net was slightly looser just after 10 W and, with some residuals of fiber pieces, looked more like that of ABS (Figure 2d–f). Similarities between PRI and ABS were also found with regard to the fiber diameter, which was found to be about $11.7 \pm 2.1 \mu\text{m}$ for PRI and about $10.6 \pm 2.3 \mu\text{m}$ for ABS. Concerning the Cu-based antibacterial treatment of the PRI sample, the Cu mass fraction was relatively low but almost constant after the repeated washing cycles (0 W: $\approx 0.35\%$; 3 W: $\approx 0.30\%$; 10 W: $\approx 0.25\%$) (Table 2).

The effect of washing and drying cycles on fibers' shape, diameter, and organization was also evaluated by SEM. In particular, fibers gradually deformed, broke up, became thicker, and aggregated accordingly with washing and drying cycles, as was also reported in the literature [41,42].

3.2. Crystalline Structures Investigation

XRD analyses of the two prototypal (SIL and COP) and two commercial (OLV and RES) antibacterial face mask fabrics were investigated to understand the crystalline nature of the fabrics and the nanomaterials present in the fabrics. Figure 4 showed the XRD pattern of the selected samples before washing and after ten washing cycles. All samples showed PP group of peaks at lower angles [43]. The crystallinity index (C.I.) of the selected samples were calculated from the XRD pattern by dividing the crystalline peak area by the total area, as reported in Figure 4a–d. It should be noted that the C.I. values significantly reduced after washing cycles, particularly for the commercial fabrics, indicating their structural damage after the washing cycles. SIL showed diffraction peaks due to mixed metallic Ag and Ag_2O [22,39,44] with not significantly reduced intensity after the washing cycles. COP showed the presence of metallic Cu [44]. The commercial OLV and RES showed the presence of a mixture of copper oxides ($\text{CuO}/\text{Cu}_2\text{O}$) and Cu [38]. In all the copper-based samples, after 10 washing cycles, the diffraction peaks due to the metal/metal oxide nanoparticles drastically decreased, indicating their loss due to several washings, as was also highlighted by SEM/EDS analysis.

3.3. Hydrophobicity Degree

Static contact angle measurements were performed in order to assess masks' degree of hydrophobicity. The prototypal masks and most of the commercial masks (OLV, ARG, RES) were characterized by a hydrophobic character ($\theta > 90^\circ$) (Table 3) [15,40]. Similar results were indeed registered for Ag- and Cu-impregnated PP fabrics [12,15]. Only ABS and PRI were characterized by strong hydrophilic character ($\theta < 90^\circ$), instantly absorbing water drops. The application of the Ag and Cu treatments on the PP fabric led to a reduction of the surface hydrophobicity ($p = 0.0007$, $p = 0.0004$ respectively). In particular, the Cu treatment reduced the hydrophobicity of COP slightly more than the treatment with Ag on SIL ($p = 0.04$). ARG and RES were found to have a contact angle value very similar to prototypal masks ($p > 0.05$), while that of OLV was significantly lower ($p < 0.05$).

The effect of washing and drying cycles was also investigated. Although a general decrease of surface hydrophobicity seemed to be observed, the differences between 3 W and 10 W were not statistically significant ($p > 0.5$).

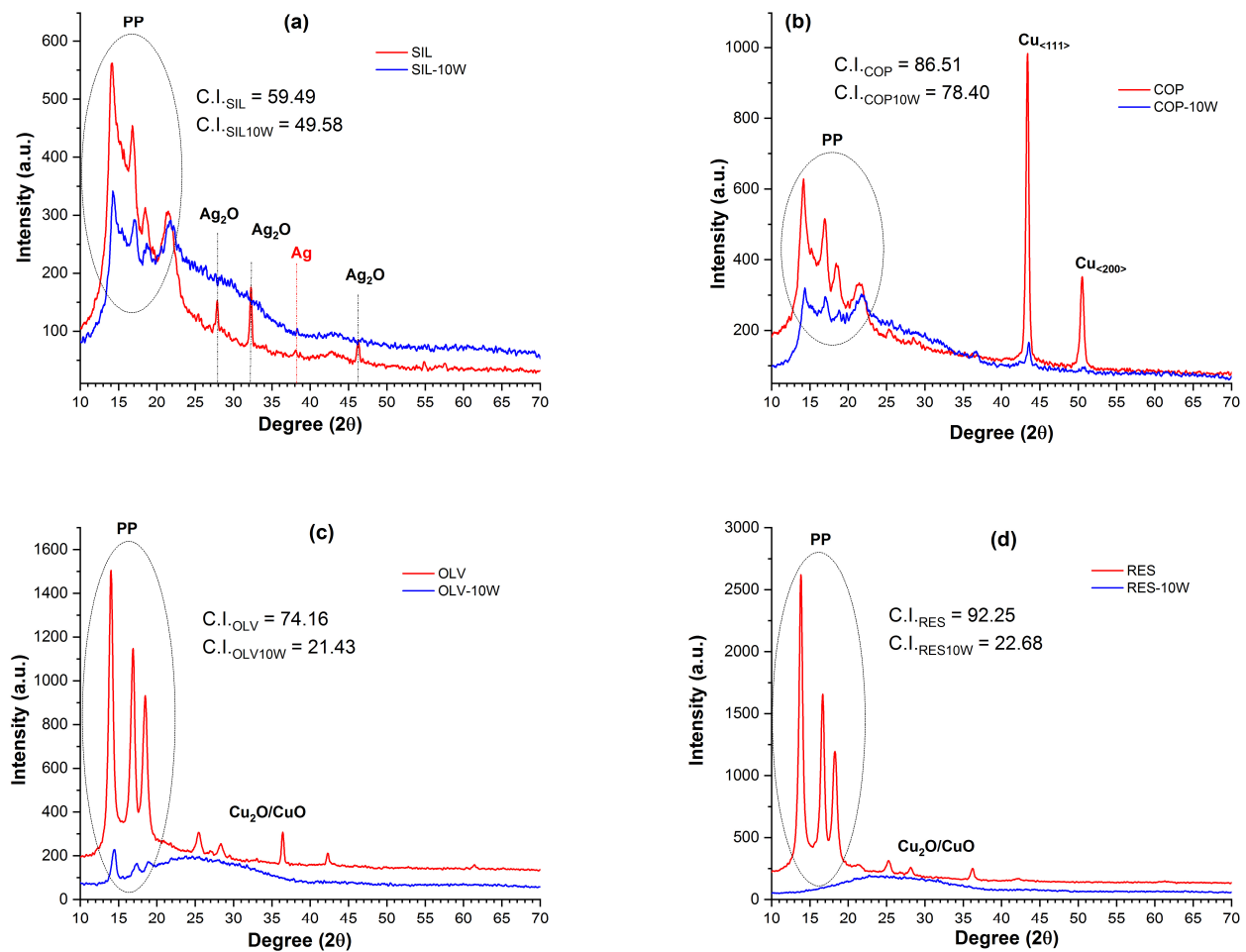


Figure 4. XRD patterns of the prototypal SIL (a) and COP (b) and of the commercial OLV (c) and RES (d).

Table 3. Contact angle values of prototypal and commercial antibacterial fabric before and after washing cycles. Values indicated represent mean \pm SD, where $n = 3$.

Mask Type	0 W	3 W	10 W
PP	134 \pm 2°	117 \pm 11°	103 \pm 4°
SIL	127 \pm 2°	110 \pm 15°	104 \pm 4°
COP	124 \pm 6°	122 \pm 3°	118 \pm 7°
OLV	104 \pm 10°	120 \pm 5°	114 \pm 4°
ARG	128 \pm 13°	118 \pm 9°	122 \pm 10°
RES	129 \pm 7°	119 \pm 8°	117 \pm 8°
ABS	0 \pm 0°	0 \pm 0°	0 \pm 0°
PRI	0 \pm 0°	0 \pm 0°	0 \pm 0°

3.4. Antibacterial Agent Content

The Ag or Cu content of masks was investigated to correlate the quantity of nanoparticles with masks' antibacterial activity. As reported in Table 4, COP had the highest Cu content, followed by OLV, RES, and lastly PRI. Commercial OLV and RES were revealed to have very similar Cu contents. Similarly, SIL had the highest Ag content, followed by ABS and ARG, whose contents were comparable. These results were partially in agreement with the literature since some studies reported similar Ag or Cu contents to our study [38,39], while others used very high antibacterial agent concentrations [12]. Washing and drying cycles induced a partial loss of Ag or Cu nanoparticles in most of the masks. In particular, while SIL and COP lost about 10% and 12% of the Ag and Cu contents, respectively, after

3 W but remained stable after 10 W, the commercial masks lost about 20–50% of antibacterial agent content after 3 W, then stabilized or further lost about 10–20% of the Ag or Cu content at 10 W.

Table 4. Gravimetrically determined Ag/Cu content (Wt%) of prototypal and commercial antibacterial fabric before and after washing cycles. Values indicated represent mean \pm SD, where $n = 3$.

Mask Type	0 W	3 W	10 W
SIL	4.0 \pm 0.7	3.6 \pm 0.6	3.6 \pm 0.3
COP	4.5 \pm 1.4	4.0 \pm 0.4	2.1 \pm 0.9
OLV	3.8 \pm 0.3	3.0 \pm 1.1	2.7 \pm 0.7
ARG	0.4 \pm 0.2	0.2 \pm 0.1	0.2 \pm 0.1
RES	3.5 \pm 0.6	2.3 \pm 0.9	2.0 \pm 0.3
ABS	0.9 \pm 0.2	0.7 \pm 0.5	0.5 \pm 0.2
PRI	1.5 \pm 0.8	1.1 \pm 0.4	0.8 \pm 0.5

3.5. Antibacterial Activity

The antibacterial power of prototypal and commercial fabrics was assessed and compared after 1 h of incubation time with *E. coli* and *S. aureus* bacterial strains. As expected, all fabrics showed the ability to reduce both bacterial titer (Figures 5 and 6). In particular, regarding the Gram-negative *E. coli*, SIL (99.9 \pm 0.2%), COP (100.0 \pm 0.0%), OLV (99.5 \pm 0.7%) [38], and RES (100.0 \pm 0.0%) were able to inhibit the bacterial proliferation almost completely, followed by ARG (87.3 \pm 3.3%), PRI (85.2 \pm 13.0%) and lastly by ABS (56.6 \pm 21.0%) (Figures S1). Regarding the Gram-positive *S. aureus* response, they did not survive SIL, COP, OLV, PRI, and RES exposure, and their proliferation was partially reduced in the presence of ARG (91.9 \pm 9.8%) and ABS (86.4 \pm 2.5%) (Figures S4). Thus, ABS, PRI, and ARG revealed stronger Gram-positive bacteria inhibition potential. The Ag-based treatment performed on SIL was revealed to be effective and confirmed the potential of silver in PP fabric functionalization that was reported in other works through different technologies [22,39]. The Cu-based treatment of COP seemed to be more effective than the one developed by Jardón-Maximino et al. since 100% of bacterial inhibition was obtained only after 1 h exposure with reduced Cu content [45]. On the contrary, photoactive Cu nanoparticles deposited on PP fabrics revealed an impressive ~ 4 log ($>99.99\%$) reduction for *E. coli* in the presence of light [12]. However, the lack of data about the antibacterial agent effective content in the fabric did not allow us to correlate the antibacterial activity with the Cu amount.

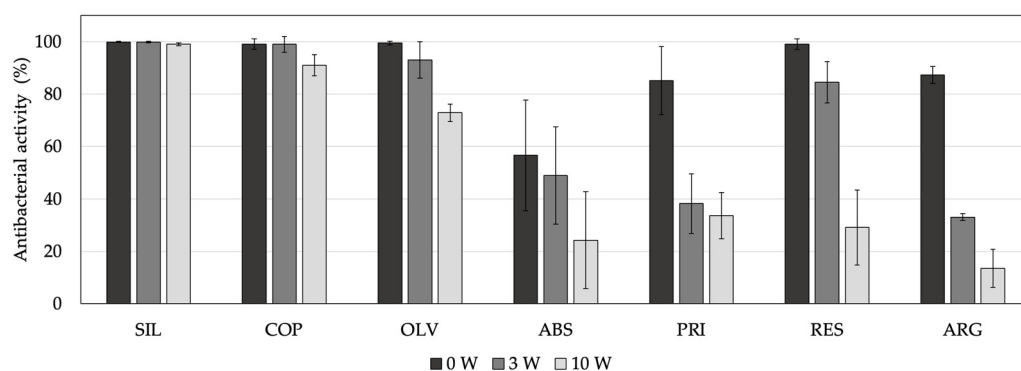


Figure 5. Percentage reduction of the antibacterial activity of prototypal and commercial fabrics before (black) and after 3 W (dark gray) and 10 W (light gray), after 1 h of incubation with 4×10^6 CFU/mL *E. coli* suspension. Values indicated represent mean \pm SD, where $n = 4$.

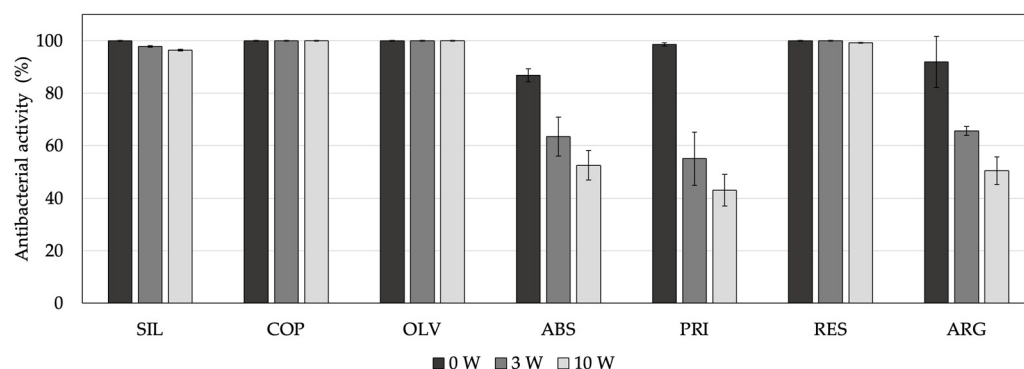


Figure 6. Percentage reduction of the antibacterial activity of prototypal and commercial fabric before (black) and after 3 W (dark gray) and 10 W (light gray), after 1 h of incubation with 4×10^6 CFU/mL *S. aureus* suspension. Values indicated represent mean \pm SD, where $n = 4$.

The antibacterial activity of fabrics was evaluated also after 3 W and 10 W to assess the efficacy of treatments over time. For some materials, according to other analyses, the bacterial proliferation reduction ability was found to decrease with washing cycles due to the gradual antibacterial agent loss. In the case of Gram-negative bacteria, the antibacterial activity was reduced to $91.0 \pm 4.1\%$ for COP, $72.9 \pm 3.3\%$ for OLV, $24.2 \pm 18.4\%$ for ABS, $33.6 \pm 8.8\%$ for PRI, $29.0 \pm 14.3\%$ for RES, and $13.5 \pm 7.3\%$ for ARG. Only SIL did not exhibit significant differences, with 100.0% antibacterial activity before washings and 99.8% after the washing cycles. This result further confirmed the strong adhesion of the coating to the substrate, which is consistent with the EDX data, and the antibacterial agent content determined by gravimetric analysis. In the case of Gram-positive bacteria, the antibacterial power was not lost after 10 W for most of the masks. In particular, SIL, COP, OLV [38], and RES activity remained almost unchanged. Instead, ABS, PRI, and ARG activity decreased with washing and drying cycles by up to $52.5 \pm 5.6\%$, $43.0 \pm 6.0\%$, and $50.5 \pm 5.3\%$, respectively.

4. Discussion

Pushed by the outbreak associated with COVID-19, the demand for new strategies to improve masks' or other medical textile materials' safety level, use time, and disposal costs has exponentially attracted interest. The high renewal rate, together with the strong environmental impact of the non-biodegradable materials of which they are composed, highlights the need to find solutions to this emerging ecological problem [3,9,10]. Among several approaches, the addition of an antimicrobial agent could not only increase masks' safety level but also limit their daily use and disposal, making them eco-friendlier and more effective.

In this work, with the aim of improving commercial devices' efficacy and eco-sustainability, Ag-based and Cu-based antibacterial treatments were developed and performed on PP fabric, the most commonly used material for the development of masks. The two prototypes we developed were characterized from morphological, compositional, chemical–physical, and microbiological points of view over time and compared with the antibacterial treatments of selected commercial products of MD (i.e., OLV), PPE (i.e., ARG, RES), and CFC (i.e., ABS, PRI).

In particular, the Ag-based treatment was performed by using a versatile technology that was successfully applied on a wide range of natural and synthetic substrates for biomedical applications, including textile materials and medical devices such as surgical sutures, wound dressings, and catheters. The technology, which is based on an in situ photochemical deposition of silver clusters onto the surface of the material, is characterized by the strong adhesion of the coating to the surface of the material and by long-term antimicrobial efficacy [16,25–28]. Indeed, even after many aging tests, including TABER tests for natural and synthetic leather, washings for textile materials, and simulated flowing condi-

tions for catheters, the silver coatings still demonstrated their efficacy on Gram-positive and Gram-negative bacteria and fungi [16,25–28]. Moreover, recent studies have given attention to the virucidal action of silver against coronaviruses [46,47], thus further increasing the interest of the scientific community toward novel silver-based nanotechnology approaches for the prevention of cross-transmission in public environments. In this work, for the specific materials and application, the process parameters were selected in order to achieve a good cost-effectiveness ratio for the potential scale-up of the process.

All analyses confirmed that the antibacterial treatments were successfully performed on both SIL and COP PP fibers of about $5.0 \pm 2.7 \mu\text{m}$ diameter. SIL was characterized by diffraction peaks due to mixed metallic Ag and Ag_2O , whereas COP was characterized by the presence of metallic Cu. Ag and Cu cluster contents of about $\approx 2.6\%$ and $\approx 6.4\%$ were, respectively, detected by EDS, while $4.0 \pm 0.7\%$ and $4.5 \pm 1.4\%$ were respectively gravimetrically determined. Great differences were evidenced in comparison with commercial masks. The MD OLV was characterized by a randomly oriented fiber net with diameters of about $15.4 \pm 1.0 \mu\text{m}$ and a uniform Cu cluster distribution of a mixture of copper oxides ($\text{CuO}/\text{Cu}_2\text{O}$) and Cu on about $\approx 0.9\%$ of the total C content (Cu content = $3.8 \pm 0.3\%$, gravimetrically determined). The PPEs, RES, and ARG were shown to be deeply different. The external layers of RES appeared to be similar to that of OLV, with fibers of about $15.8 \pm 0.8 \mu\text{m}$, a homogeneous distribution of $\text{CuO}/\text{Cu}_2\text{O}$, and Cu clusters on $\approx 1.6\%$ of the total C. Almost the same gravimetric content of Cu was detected, with a total of $3.5 \pm 0.6\%$. Conversely, the inner layer of ARG was characterized by a looser net of bigger fibers of about $26.4 \pm 2.7 \mu\text{m}$, with a very low Ag content ($\approx 0.24\%$ from EDS, $0.4 \pm 0.2\%$ from the incineration method). The CFCs, ABS, and PRI were instead revealed to be similarly characterized by a woven texture with fibers of about $10.6 \pm 2.3 \mu\text{m}$ for ABS and $11.7 \pm 2.1 \mu\text{m}$ for PRI. Concerning the antibacterial agent content, the presence of relatively small Ag and Cu nanoparticles was highlighted, which were respectively identified as $\approx 1.0\%$ and $\approx 0.3\%$ of the C mass fraction from EDS and $0.9 \pm 0.2\%$ and $1.5 \pm 0.8\%$ from the gravimetric analysis. However, because of the very low content of antibacterial agents on ARG, ABS, and PRI, the crystalline nature of Ag or Cu nanoparticles was not revealed. Static contact angle measurements showed that the prototypal masks (SIL and COP) and most of the commercial masks (OLV, ARG, RES) showed a hydrophobic character. Only ABS, PRI were characterized by a strong hydrophilic character, instantly absorbing water drops. The antibacterial power of the fabrics were assessed and compared after 1 h of incubation with Gram-negative or Gram-positive bacteria. All the produced (or received) fabrics showed the ability to reduce both bacterial titers. In particular, SIL, COP, OLV, and RES were able to almost completely inhibit *E. coli* growth, followed by ARG ($87.3 \pm 3.3\%$), PRI ($85.2 \pm 13.0\%$), and ABS ($56.6 \pm 21.0\%$). Similarly, SIL, COP, OLV, RES, and PRI were able to almost completely restrain *S. aureus* proliferation, while ARG ($91.9 \pm 9.8\%$) and ABS ($86.4 \pm 2.5\%$) restrained it a little bit less.

Although the mask substrates used for antibacterial treatments were disposable, the impact of washing and drying cycles was evaluated on all experimental classes in order to evaluate the durability of materials and coatings. Regardless of the treatments, in all conditions, fibers were found to gradually deform, break up, become thicker, and aggregate accordingly with washing and drying cycles. This effect was clearly visible in both the SIL and COP prototypal fabrics and in the commercial masks. This result was in line with the study of Whyte et al., who reported that after 20 washings, PP fabric fibers became slightly deconstructed and were no longer able to filter submicron particles [41]. Similarly, Varanges et al. reported a non-uniform fiber distribution and a larger pore size compared to the reference, which was found to be the cause of the increase in air permeability [42].

Moreover, differences in Ag and Cu cluster distribution were detected before and after washing cycles. In particular, the SIL coating was not significantly affected by the washing cycles, which was also noted by the elemental analysis, the residual Ag content, and the X-ray analysis data. In COP, about $2.1 \pm 0.9\%$ of Cu ($\approx 0.16\%$ Cu/C) remained on the PP fabric. In the cases of ARG, ABS, and PRI, the low initial amount of Ag or Cu

further decreased to less than 1%. Conversely, RES and OLV's fiber morphology and Cu nanoparticle content remained almost completely unvaried even after 10 washing cycles, as confirmed by the elemental decrease in Cu content of about 0.1% for OLV and about 0.8% for RES and the gravimetric decrease 1.0–1.5% for both. According to the elemental and gravimetric analyses, samples' diffraction peak intensity decreased according to washing and drying cycles, indicating their losses. The antibacterial activity of the fabrics was also evaluated after 3 W and 10 W to assess the efficacy of the treatments over time. The gradual loss of the antibacterial agent during washing and drying cycles was responsible for the progressive loss of their bacterial proliferation reduction ability for most of the samples. However, all masks retained their antibacterial potential after 10 W proportionally to their Ag or Cu residual content, suggesting that the addition of an antimicrobial agent on MDs, PPEsm or CFCs could increase masks' safety level over time, limit their daily use, and reduce disposal costs, making them not only more effective but also eco-friendlier.

Although these preliminary studies had positive outcomes, further research should be done to investigate the performances of the prototypes after accurate aging tests, aiming to simulate masks folding and exposure to body fluids in addition to air flow. Last but not least, permeability, mechanical integrity, electrostatic potential, and bacterial/viral filtration efficiency are intended to be the next characterizations to assess the safety and effectiveness of the developed prototypes.

Supplementary Materials: The following supporting information can be downloaded at: <https://www.mdpi.com/article/10.3390/coatings13050919/s1>, Figure S1: Growth plate of *E. coli* after incubation with PP, SIL and COP; Figure S2: Growth plate of *E. coli* after incubation with ARG and ABS; Figure S3: Growth plate of *E. coli* after incubation with OLV, RES and PRI; Figure S4: Growth plate of *S. aureus* after incubation with PP, SIL and COP; Figure S5: Growth plate of *S. aureus* after incubation with ARG and ABS; Figure S6: Growth plate of *S. aureus* after incubation with OLV, RES and PRI.

Author Contributions: Conceptualization, M.P., F.P., S.P. and L.S.; methodology, N.G., G.N.I., S.P., M.P. and F.P.; software, S.P. and C.N.; validation, N.G., G.N.I., M.P., F.P., S.P. and C.N.; formal analysis, N.G., S.P. and C.N.; investigation, N.G., G.N.I., M.P., S.P. and C.N.; resources, A.S., A.L., M.P., L.C. and L.S.; data curation, N.G., G.N.I., F.P., S.P. and C.N.; writing—original draft preparation, N.G., G.N.I., S.P. and C.N.; writing—review and editing, F.P., L.C., A.L., L.S. and A.S.; visualization, N.G., G.N.I., C.N. and S.P.; supervision, A.S., L.S., G.G.B., A.M., L.C. and A.L.; project administration, A.S., A.L., G.G.B., A.M. and L.S.; funding acquisition, A.S. All authors have read and agreed to the published version of the manuscript.

Funding: This research was funded by the project “NANOBIOSAN: Materiali NANOstrutturati per la prevenzione del rischio BIOlogico: dalla progettazione alla verifica di applicabilità ed efficacia in ambito SANitario” (CUP: B64I20000010005).

Institutional Review Board Statement: Not applicable.

Informed Consent Statement: Not applicable.

Data Availability Statement: Not applicable.

Acknowledgments: This research was funded by INAIL within the framework of the project BRIC 2019-ID49 “NANOBIOSAN: Materiali NANOstrutturati per la prevenzione del rischio BIOlogico: dalla progettazione alla verifica di applicabilità ed efficacia in ambito SANitario” (CUP: B64I20000010005).

Conflicts of Interest: The authors declare no conflict of interest. The funders had no role in the design of the study; in the collection, analyses, or interpretation of data; in the writing of the manuscript; or in the decision to publish the results.

References

1. Liao, M.; Liu, H.; Wang, X.; Hu, X.; Huang, Y.; Liu, X.; Brenan, K.; Mecha, J.; Nirmalan, M.; Lu, J.R. A Technical Review of Face Mask Wearing in Preventing Respiratory COVID-19 Transmission. *Curr. Opin. Colloid. Interface Sci.* **2021**, *52*, 101417. [CrossRef] [PubMed]
2. Tirupathi, R.; Bharathidasan, K.; Palabindala, V.; Salim, S.A.; Al-Tawfiq, J.A. Comprehensive Review of Mask Utility and Challenges during the COVID-19 Pandemic. *Infez. Med.* **2020**, *28*, 57–63. [PubMed]
3. Selvaranjan, K.; Navaratnam, S.; Rajeev, P.; Ravintherakumaran, N. Environmental Challenges Induced by Extensive Use of Face Masks during COVID-19: A Review and Potential Solutions. *Environ. Chall.* **2021**, *3*, 100039. [CrossRef]
4. UNI EN 14683:2019 – Maschere Facciali Ad Uso Medico-Requisiti e Metodi Di Prova. Available online: https://store.uni.com/catalogo/uni-en-14683-2019-292195?josso_back_to=https://store.uni.com/josso-security-check.php&josso_cmd=login_optional&josso_partnerapp_host=store.uni.com (accessed on 6 April 2022).
5. UNI EN 149:2009 – Dispositivi Di Protezione Delle Vie Respiratorie-Semimaschere Filtranti Antipolvere-Requisiti, Prove, Marcatura. Available online: <https://store.uni.com/catalogo/uni-en-149-2009> (accessed on 6 April 2022).
6. PdR UNI 90:2020—Maschere Di Comunità. Available online: <https://store.uni.com/uni-pdr-90-1-2020> (accessed on 6 April 2022).
7. Pullangott, G.; Kannan, U.; Gayathri, S.; Kiran, D.V.; Maliyekkal, S.M. A Comprehensive Review on Antimicrobial Face Masks: An Emerging Weapon in Fighting Pandemics. *RSC Adv.* **2021**, *11*, 6544–6576. [CrossRef]
8. Xu, E.G.; Ren, Z.J. Preventing Masks from Becoming the next Plastic Problem. *Front. Environ. Sci. Eng.* **2021**, *15*, 6–8. [CrossRef]
9. Hu, T.; Shen, M.; Tang, W. Wet Wipes and Disposable Surgical Masks Are Becoming New Sources of Fiber Microplastic Pollution during Global COVID-19. *Environ. Sci. Pollut. Res.* **2022**, *29*, 284–292. [CrossRef]
10. Chen, X.; Chen, X.; Liu, Q.; Zhao, Q.; Xiong, X.; Wu, C. Used Disposable Face Masks Are Significant Sources of Microplastics to Environment. *Environ. Pollut.* **2021**, *285*, 117485. [CrossRef]
11. Aboubakr, H.A.; Sharafeldin, T.A.; Goyal, S.M. Stability of SARS-CoV-2 and Other Coronaviruses in the Environment and on Common Touch Surfaces and the Influence of Climatic Conditions: A Review. *Transbound. Emerg. Dis.* **2021**, *68*, 296–312. [CrossRef]
12. Valdez-Salas, B.; Beltran-Partida, E.; Cheng, N.; Salvador-Carlos, J.; Valdez-Salas, E.A.; Curiel-Alvarez, M.; Ibarra-Wiley, R. Promotion of Surgical Masks Antimicrobial Activity by Disinfection and Impregnation with Disinfectant Silver Nanoparticles. *Int. J. Nanomed.* **2021**, *16*, 2689–2702. [CrossRef]
13. Blevens, M.S.; Pastrana, H.F.; Mazzotta, H.C.; Tsai, C.S.-J. Cloth Face Masks Containing Silver: Evaluating the Status. *ACS Chem. Health Saf.* **2021**, *28*, 171–182. [CrossRef]
14. Borkow, G.; Melamed, E. Copper, an Abandoned Player Returning to the Wound Healing Battle. *Recent. Adv. Wound Health* **2022**. [CrossRef]
15. Kumar, S.; Karmacharya, M.; Joshi, S.R.; Gulenko, O.; Park, J.; Kim, G.-H.; Cho, Y.-K. Photoactive Antiviral Face Mask with Self-Sterilization and Reusability. *Nano Lett.* **2021**, *21*, 337–343. [CrossRef] [PubMed]
16. Picca, R.A.; Paladini, F.; Sportelli, M.C.; Pollini, M.; Giannossa, L.C.; Di Franco, C.; Panico, A.; Mangone, A.; Valentini, A.; Cioffi, N. Combined Approach for the Development of Efficient and Safe Nanoantimicrobials: The Case of Nanosilver-Modified Polyurethane Foams. *ACS Biomater. Sci. Eng.* **2017**, *3*, 1417–1425. [CrossRef]
17. Alexander, J.W. History of the Medical Use of Silver. *Surg. Infect.* **2009**, *10*, 289–294. [CrossRef]
18. Dollwet, H.H.A.; Sorenson, J.R.J. Historic Uses of Copper Compounds in Medicine. *Trace Elem. Med.* **1985**, *2*, 80–87.
19. Jung, S.; Yang, J.-Y.; Byeon, E.-Y.; Kim, D.-G.; Lee, D.-G.; Ryoo, S.; Lee, S.; Shin, C.-W.; Jang, H.W.; Kim, H.J.; et al. Copper-Coated Polypropylene Filter Face Mask with SARS-CoV-2 Antiviral Ability. *Polymers* **2021**, *13*, 1367. [CrossRef] [PubMed]
20. Borkow, G.; Gabbay, J. Copper as a Biocidal Tool. *Curr. Med. Chem.* **2005**, *12*, 2163–2175. [CrossRef]
21. Gomes, I.B.; Simões, M.; Simões, L.C. Copper Surfaces in Biofilm Control. *Nanomaterials* **2020**, *10*, 2491. [CrossRef] [PubMed]
22. Hiragond, C.B.; Kshirsagar, A.S.; Dhapte, V.V.; Khanna, T.; Joshi, P.; More, P.V. Enhanced Anti-Microbial Response of Commercial Face Mask Using Colloidal Silver Nanoparticles. *Vacuum* **2018**, *156*, 475–482. [CrossRef]
23. Borkow, G.; Okon-Levy, N.; Gabbay, J. Copper Oxide Impregnated Wound PL. *Wounds* **2010**, *22*, 301–310.
24. Sportelli, M.C.; Picca, R.A.; Ronco, R.; Bonerba, E.; Tantillo, G.; Pollini, M.; Sannino, A.; Valentini, A.; Cataldi, T.R.I.; Cioffi, N. Investigation of Industrial Polyurethane Foams Modified with Antimicrobial Copper Nanoparticles. *Materials* **2016**, *9*, 544. [CrossRef] [PubMed]
25. Pollini, M.; Paladini, F.; Licciulli, A.; Maffezzoli, A.; Sannino, A. Engineering Nanostructured Silver Coatings for Antimicrobial Applications. In *Nano-Antimicrobials*; Springer: Berlin/Heidelberg, Germany, 2012; pp. 313–336.
26. Cooper, I.R.; Pollini, M.; Paladini, F. The Potential of Photo-Deposited Silver Coatings on Foley Catheters to Prevent Urinary Tract Infections. *Mater. Sci. Eng. C* **2016**, *69*, 414–420. [CrossRef] [PubMed]
27. Sportelli, M.C.; Picca, R.A.; Paladini, F.; Mangone, A.; Giannossa, L.C.; Franco, C.D.; Gallo, A.L.; Valentini, A.; Sannino, A.; Pollini, M.; et al. Spectroscopic Characterization and Nanosafety of Ag-Modified Antibacterial Leather and Leatherette. *Nanomaterials* **2017**, *7*, 203. [CrossRef]
28. Raho, R.; Paladini, F.; Lombardi, F.A.; Boccarella, S.; Zunino, B.; Pollini, M. In-Situ Photo-Assisted Deposition of Silver Particles on Hydrogel Fibers for Antibacterial Applications. *Mater. Sci. Eng. C* **2015**, *55*, 42–49. [CrossRef] [PubMed]
29. Sagripanti, J.-L.; Goering, P.L.; Lamanna, A. Interaction of Copper with DNA and Antagonism by Other Metals. *Toxicol. Appl. Pharmacol.* **1991**, *110*, 477–485. [CrossRef] [PubMed]

30. Arendsen, L.P.; Thakar, R.; Sultan, A.H. The Use of Copper as an Antimicrobial Agent in Health Care, Including Obstetrics and Gynecology. *Clin. Microbiol. Rev.* **2019**, *32*, e00125–18. [[CrossRef](#)]
31. Salah, I.; Parkin, I.P.; Allan, E. Copper as an Antimicrobial Agent: Recent Advances. *RSC Adv.* **2021**, *11*, 18179–18186. [[CrossRef](#)]
32. Anees Ahmad, S.; Sachi Das, S.; Khatoun, A.; Tahir Ansari, M.; Afzal, M.; Saquib Hasnain, M.; Kumar Nayak, A. Bactericidal Activity of Silver Nanoparticles: A Mechanistic Review. *Mater. Sci. Energy Technol.* **2020**, *3*, 756–769. [[CrossRef](#)]
33. Yin, I.X.; Zhang, J.; Zhao, I.S.; Mei, M.L.; Li, Q.; Chu, C.H. The Antibacterial Mechanism of Silver Nanoparticles and Its Application in Dentistry. *Int. J. Nanomed.* **2020**, *15*, 2555–2562. [[CrossRef](#)]
34. Franci, G.; Falanga, A.; Galdiero, S.; Palomba, L.; Rai, M.; Morelli, G.; Galdiero, M. Silver Nanoparticles as Potential Antibacterial Agents. *Molecules* **2015**, *20*, 8856–8874. [[CrossRef](#)]
35. Morones, J.R.; Elechiguerra, J.L.; Camacho, A.; Holt, K.; Kouri, J.B.; Ramírez, J.T.; Yacaman, M.J. The Bactericidal Effect of Silver Nanoparticles. *Nanotechnology* **2005**, *16*, 2346–2353. [[CrossRef](#)]
36. Silvia, G.; Pagani, I.; Poli, G.; Pal, S.; Licciulli, A.; Perboni, S.; Vicenzi, E. Rapid Inactivation of SARS-CoV-2 by Coupling Tungsten Trioxide (WO₃) Photocatalyst with Copper Nanoclusters. *J. Nanotechnol. Nanomater.* **2020**, *1*, 109–115. [[CrossRef](#)]
37. Gallo, N.; Natali, M.L.; Curci, C.; Picerno, A.; Gallone, A.; Vulpi, M.; Vitarelli, A.; Ditunno, P.; Cascione, M.; Sallustio, F.; et al. Analysis of the Physico-Chemical, Mechanical and Biological Properties of Crosslinked Type-I Collagen from Horse Tendon: Towards the Development of Ideal Scaffolding Material for Urethral Regeneration. *Materials* **2021**, *14*, 7648. [[CrossRef](#)] [[PubMed](#)]
38. Borkow, G.; Salvatori, R.; Kanmukhla, V.K. Drastic Reduction of Bacterial, Fungal and Viral Pathogen Titers by Cuprous Oxide Impregnated Medical Textiles. *J. Funct. Biomater.* **2021**, *12*, 9. [[CrossRef](#)]
39. Gawish, S.M.; Mosleh, S. Antimicrobial Polypropylene Loaded by Silver Nano Particles. *Fibers Polym.* **2020**, *21*, 19–23. [[CrossRef](#)]
40. Zhu, S.; Kang, Z.; Wang, F.; Long, Y. Copper Nanoparticle Decorated Non-Woven Polypropylene Fabrics with Durable Superhydrophobicity and Conductivity. *Nanotechnology* **2021**, *32*, 035701. [[CrossRef](#)]
41. Whyte, H.E.; Joubert, A.; Leclerc, L.; Sarry, G.; Verhoeven, P.; Le Coq, L.; Pourchez, J. Reusability of Face Masks: Influence of Washing and Comparison of Performance between Medical Face Masks and Community Face Masks. *Environ. Technol. Innov.* **2022**, *28*, 102710. [[CrossRef](#)]
42. Varanges, V.; Caglar, B.; Lebaupin, Y.; Batt, T.; He, W.; Wang, J.; Rossi, R.M.; Richner, G.; Delaloye, J.-R.; Michaud, V. On the Durability of Surgical Masks after Simulated Handling and Wear. *Sci. Rep.* **2022**, *12*, 4938. [[CrossRef](#)]
43. Cho, D.; Zhou, H.; Cho, Y.; Audus, D.; Joo, Y.L. Structural Properties and Superhydrophobicity of Electrospun Polypropylene Fibers from Solution and Melt. *Polymer* **2010**, *51*, 6005–6012. [[CrossRef](#)]
44. Chu, C.; Hu, X.; Yan, H.; Sun, Y. Surface Functionalization of Nanostructured Cu/Ag-Deposited Polypropylene Fiber by Magnetron Sputtering. *e-Polymers* **2021**, *21*, 140–150. [[CrossRef](#)]
45. Jardón-Maximino, N.; Cadenas-Pliego, G.; Ávila-Orta, C.A.; Comparán-Padilla, V.E.; Lugo-Urbe, L.E.; Pérez-Alvarez, M.; Tavizón, S.F.; Santillán, G.d.J.S. Antimicrobial Property of Polypropylene Composites and Functionalized Copper Nanoparticles. *Polymers* **2021**, *13*, 1694. [[CrossRef](#)] [[PubMed](#)]
46. Balagna, C.; Perero, S.; Percivalle, E.; Nepita, E.V.; Ferraris, M. Virucidal Effect against Coronavirus SARS-CoV-2 of a Silver Nanocluster/Silica Composite Sputtered Coating. *Open. Ceram.* **2020**, *1*, 100006. [[CrossRef](#)]
47. Lv, X.; Wang, P.; Bai, R.; Cong, Y.; Suo, S.; Ren, X.; Chen, C. Inhibitory Effect of Silver Nanomaterials on Transmissible Virus-Induced Host Cell Infections. *Biomaterials* **2014**, *35*, 4195–4203. [[CrossRef](#)] [[PubMed](#)]

Disclaimer/Publisher’s Note: The statements, opinions and data contained in all publications are solely those of the individual author(s) and contributor(s) and not of MDPI and/or the editor(s). MDPI and/or the editor(s) disclaim responsibility for any injury to people or property resulting from any ideas, methods, instructions or products referred to in the content.